Molecular Crystals and Liquid Crystals Incorporating Nonlinear Optics

Publication details, including instructions for authors and subscription information:
http://www.tandfonline.com/loi/gmcl17

Optical Constants of Tetracene Single Crystal within the First Absorption Band

J. Kalinowski [a] , J. Godlewski [a] , S. Stizza [b] , I. Davoli [b] & G. Manchini [b]

[a] Department of Molecular Physics, Technical University of Gdansk, 80-952, Gdansk, Poland

[b] Department of Mathematics and Physics, University of Camerino, 62 032, Camerino, Italy

Version of record first published: 22 Sep 2006.

To cite this article: J. Kalinowski , J. Godlewski , S. Stizza , I. Davoli & G. Manchini (1989): Optical Constants of Tetracene Single Crystal within the First Absorption Band, Molecular Crystals and Liquid Crystals Incorporating Nonlinear Optics, 166:1, 233-244

To link to this article: http://dx.doi.org/10.1080/00268948908037152

Mol. Cryst. Liq. Cryst., 1989, Vol. 166, pp. 233–244
Reprints available directly from the publisher
Photocopying permitted by license only

Printed in the United States of America

Optical Constants of Tetracene Single Crystal within the First Absorption Band†

J. KALINOWSKI and J. GODLEWSKI

Department of Molecular Physics, Technical University of Gdansk, 80-952 Gdansk, Poland

and

S. STIZZA, I. DAVOLI and G. MANCINI

Department of Mathematics and Physics, University of Camerino, 62 032 Camerino, Italy

(*Received March 9, 1988*)

Optical constants of tetracene single crystal within the first absorption band have been determined for various polarization states of the light incident on its crystallographic (*ab*) plane at room temperature. A method based on the combination of the reflectance spectra taken from the crystal interface with two different transparent media (TTM method) has been developed in order to avoid approximations needed for the analysis by usual Kramers-Kronig (KK) method. In contrast to the latter, our method does not require the knowledge of the reflectivity throughout the entire energy range and a comparison of the results with independent experimental absorption and refraction data of the crystal shows the method to be more accurate than KK method.

Some possible applications of the data are briefly discussed in conjunction with intermolecular structure of crystalline tetracene.

Keywords: optical constants, molecular constants, reflectivity

1. INTRODUCTION

Investigation of optical properties is one of the most powerful experimental methods of probing the electronic structure and properties of organic crystals.[1]

To determine optical constants of solids, reflection and absorption spectra have been usually employed in conjunction with the Kramers-Kronig dispersion relations (see e.g. Reference 2). The Kramers-Kronig relations require a knowledge of the reflectivity throughout the entire energy range. However, since the range of frequencies over which an optical quantity may be measured is necessarily limited,

†The work performed in the framework of the cooperation agreement between Technical University of Gdansk and the University of Camerino, and supported in part by the Polish Academy of Sciences under Program CPBP 01.12.

theoretical tools such as extrapolations and sum rules are needed for the analysis of optical experiments by this method (see References 3 and 4, and more recently 5 to 7).

In order to avoid inconveniences and, more important, possible distortions resulting from all these operations, we have described a method based on narrow-range reflectance spectroscopy which does not require use of Kramers-Kronig analysis. The method is applied to tetracene single crystal and the results compared with those obtained by usual Kramers-Kronig procedure.

Tetracene crystal and the first singlet transition in it have been chosen because the direct absorption spectra in this optical region with very thin tetracene flakes have been recently obtained,[8] giving a good reference to ours obtained on thick crystals indirectly.

2. DESCRIPTION OF THE METHOD

A. Physical basis

The optical properties of a dispersive isotropic solid can be described entirely by the real (ε_r) and imaginary (ε_i) parts of a complex dielectric constant ($\tilde{\varepsilon}$) connected to the electronic properties of the solid. To describe optical properties of an anisotropic crystal one has to use suitable tensors. Let us consider the case in which linearly polarized light falls perpendicularly from a transparent medium with the real refractive index n_0 on the boundary surface of a strongly absorbing crystal with the complex refractive index $\tilde{n} = (\tilde{\varepsilon})^{1/2} = n + ik$ (n, the real and k, the imaginary part of the index). The reflectivity corresponding to each dielectric tensor component is then given by the well known formula

$$R = \frac{(n - n_0)^2 + k^2}{(n + n_0)^2 + k^2} \tag{1}$$

in which n and k are related to ε_r and ε_i by

$$\varepsilon_r = n^2 - k^2, \tag{2}$$

$$\varepsilon_i = 2nk, \tag{3}$$

and to the absorption coefficient (ϵ) by

$$\epsilon = \frac{4\pi k}{\lambda}, \tag{4}$$

where λ is the wavelength of the incident light.

The method for determining $\varepsilon_r(\lambda)$ and $\varepsilon_i(\lambda)$ functions consists in measuring the $R(\lambda)$ curve with two different transparent media in contact (R_1, R_2), by solution

of the two resulting equations (1), obtaining n and k, and then using relations (2) and (3).

If one of the two media is air ($n_0 \approx 1$), n and k of the crystal can be expressed by R_1 and R_2 as follows:

$$n = \frac{n_0^2 - 1}{2\left[n_0 \dfrac{1 + R_2}{1 - R_2} - \dfrac{1 + R_1}{1 - R_1}\right]}, \tag{5}$$

$$k = \left[\frac{R_1(n + 1)^2 - (n - 1)^2}{1 - R_1}\right]^{1/2}. \tag{6}$$

B. An application to interfaces with air and a liquid

In order to use the idea given in Section 2A practically, one has to make a good optical contact between the crystal and the second transparent medium. The simplest way to do that is to put crystal into an non-solvent liquid. Then the reflectance properties of the liquid container have to be taken into account. Let the container be a parallel-plane quartz cuvette (Figure 1). The observed ratios of the light intensity (I') reflected from the empty cuvette (air) and filled with a liquid (liq) to the incident light intensity (I_0) are given by

$$R'_{\text{obs}1} = \left(\frac{I'}{I_0}\right)_{\text{air}}; \qquad R'_{\text{obs}2} = \left(\frac{I'}{I_0}\right)_{\text{liq}}. \tag{7a}$$

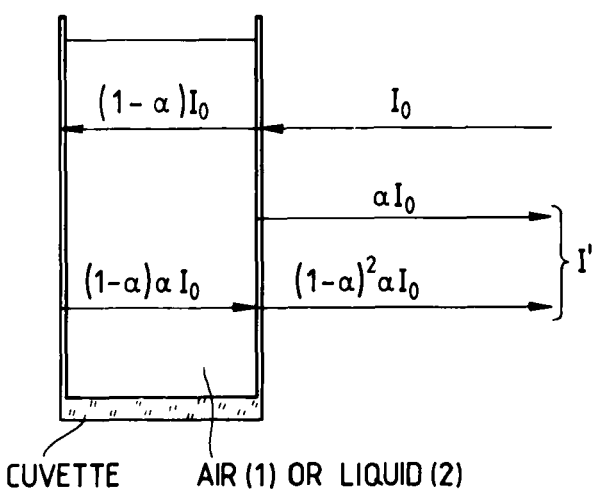

FIGURE 1 Schematic illustration of light reflection from a parallel-plane cuvette, showing the contribution to the reflectivity of its two walls (for symbol explanations see text).

Corresponding ratios with the crystal inside (see Figure 2) are

$$R''_{\text{obs}1} = \left(\frac{I''}{I_0}\right)_{\text{air}}; \qquad R''_{\text{obs}2} = \left(\frac{I''}{I_0}\right)_{\text{liq}}. \tag{7b}$$

The reflectivity of each cuvette wall itself can be obtained from (7a) and in an approximation expressed as

$$\alpha_{1,2} \approx \frac{1 - (1 - 2R'_{\text{obs}(1,2)})^{1/2}}{2}, \tag{8}$$

and then the crystal reflectivity calculated from

$$R_{1,2} = \frac{R''_{(1,2)} - \alpha_{1,2}}{(1 - \alpha_{1,2})^2}. \tag{9}$$

Due to large values of k multiple reflections in the crystal specimen have not been taken into account in this formula. It can be noticed that formula (9) yields the crystal reflectance spectrum in contact with two different media on the basis of directly measured quantities $R'_{\text{obs}(1,2)}$ and $R''_{\text{obs}(1,2)}$ containing the reflectance properties of the crystal container (cuvette).

3. EXPERIMENTAL

A tetracene single crystal is fixed on one of the internal walls of a quartz cuvette as shown in Figure 2. The optical path is represented in Figure 2 by a solid line starting from the light source. The light from a halogen lamp is focused on the

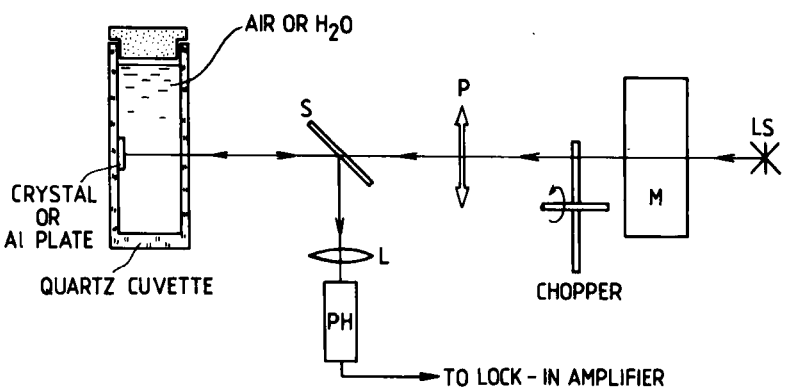

FIGURE 2 Diagram of the setup used for the measurement of crystal reflectance spectra with different media in contact. The light from the light source (LS), passed through the monochromator (M) and the polarizer (P), reflects from the crystal or Al plate and then by means of a quartz splitter (S) and a lens (L) focused on the photocathode of the photomultiplier (PH).

entrance slit of the monochromator. The resulting monochromatic beam ($\Delta\lambda \approx 4$ nm) passing the front cuvette wall is focused on the crystal sample, from which it is reflected at near-normal incidence and directed by a quartz splitter on a photomultiplier. Problems associated with instability of the light source and unstable dark current of the photomultiplier (especially at low intensities of reflected light) were to a large extent avoided by chopping the light and sending the ac signal from the photomultiplier output to a lock-in amplifier, the reference of which was supplied by the same generator that settled the modulation frequency. The overall accuracy of the measurement of the crystal reflectivity was better than 2%. For the crystal spectra expressed in absolute units the reflectance from a polished Al plate (foil) put in place of the crystal has been used as a reference.

4. RESULTS

Polarized reflectance spectra (R) of a 50 μm-thick tetracene single crystal (obtained in a way described in Section 2B) in the energy range of $S_0 \rightarrow S_1$ transition are presented in Figure 3. Two parts of this figure correspond to the reflectivity measurements on the crystal with its reflecting surface in contact with air (a) and water (b). In each case three curves are presented, the parameter is the angle between the polarization direction of light and the b axis of the crystal. Principal features of the spectra are summarized in Table I.

It can be recognized at once that the maximum reflectivity belongs to light in the polarization state ($\theta = 30°$) far from the b-polarized light to which this feature is often improperly ascribed.

The basic feature upon replacing air with water is lowering of the reflectivity and a blue shift of all the reflectance bands for light of each polarization state.

To extract quantitative information on optical constants, we subjected the experimental reflectance spectra to the procedure described in Section 2A. Guided

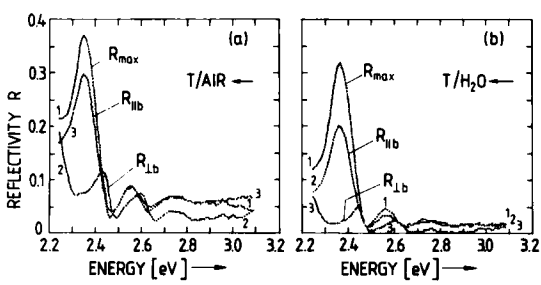

FIGURE 3 Room temperature, normal-incidence reflectance spectra of a 50 μm-thick tetracene single crystal at the interface with air (a) and water (b) with different polarization states of the incident light. The maximum reflectivity (R_{max}) is obtained with linearly polarized light, the electric vector of light making an angle 30° with the crystallographic b axis in the (ab) plane of the crystal; $R_{\|b}$ and $R_{\perp b}$ corresponds to the light polarization with the electric vector parallel and perpendicular to the b axis in the same plane, respectively.

TABLE I

Principal features of a 50 μm-thick tetracene single crystal reflectance spectra for the crystal/air and crystal/water interfaces at 295 K

Crystal/air interface			Crystal/water interface		
$\|\|b$ $\hbar\omega$[eV]	$\perp b$ $\hbar\omega$[eV]	30° with b $\hbar\omega$[eV]	$\|\|b$ $\hbar\omega$[eV]	$\perp b$ $\hbar\omega$[eV]	30° with b $\hbar\omega$[eV]
2.356 (max)	2.430 (max)	2.356 (max)	2.365 (max)	2.440 (max)	2.365 (max)
2.469 (min)	2.489 (min)	2.469 (min)	2.489 (min)	2.499 (min)	2.479 (min)
2.561 (max)	2.593 (max)	2.551 (max)	2.565 (max)	2.604 (max)	2.561 (max)
2.638 (min)	2.661 (min)	2.627 (min)	2.649 (min)	2.684 (min)	2.638 (min)
2.750 (max)	2.743 (max)	2.731 (max)	2.756 (max)	2.756 (max)	2.731 (max)

by formulae (5) and (6) we calculated n and k and then using (4) obtained absorption coefficient ϵ. The results are shown in Figure 4a.

The main features of the $\|b$ and $\perp b$ absorption (ϵ) spectra agree with the room temperature spectra reported by Bree and Lyons.[9] The maximum values of $\epsilon(\|b) = 3.6 \times 10^5\ \mathrm{cm}^{-1}$ and of $\epsilon(\perp b) = 1.5 \times 10^5\ \mathrm{cm}^{-1}$ are close to the values $\epsilon(\|b) = 4.2 \times 10^5\ \mathrm{cm}^{-1}$ and $\epsilon(\perp b) = 1.4 \times 10^5\ \mathrm{cm}^{-1}$ obtained recently by Mizuno *et al.*[8] from direct measurements on thin tetracene monocrystals. Also, the values $n(\|b) = 3$ and $n(\perp b) = 2$ within suitable spectral range are in good agreement

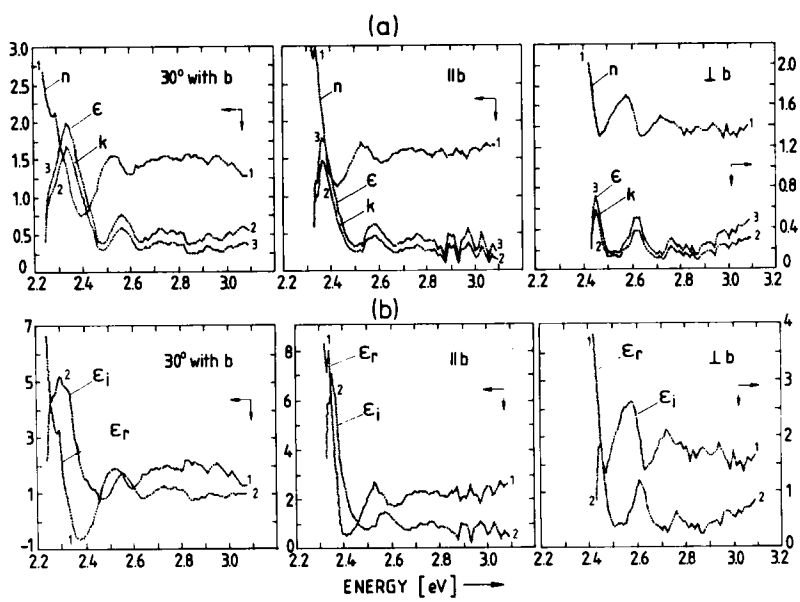

FIGURE 4 Optical constants versus photon energy for the tetracene single crystal as determined from the data of Figure 3 by the two-transparent media (TTM) method. The upper part (a): n, ϵ and k for three different light polarization states; the ordinate for ϵ must be multiplied by a factor $2 \times 10^5 \mathrm{cm}^{-1}$. The lower part ($b$): ε_i and ε_r for the three different light polarization states as in part (a) (the light polarization states as described in Figure 3). All the structures above 2.8 eV are imposed by finite resolution of the procedure for determination of the constants, and do not have other physical meaning.

with the values $n(\|b) = 2.99 \pm 0.04$ and $n(\perp b) = 2.02 \pm 0.02$ as determined by those authors from interference patterns observed in the transmittance spectra in a specimen of 19 μm at room temperature.

The optical constants ε_r and ε_i for light of three different polarization states are shown in Figure 4b as a function of photon energy. They have been calculated from (2) and (3) on the basis of data contained in Figure 4a. Figure 4b demonstrates that the maximum values of these two constants occur for a different polarization state of the incident light than those for the crystal reflectivity. Whereas R reaches its maximum for the polarization state with $\theta = 30°$ (see Figure 3), ε_r and ε_i display their maxima for $\|b$-polarized light. The reflectivity as a function of the polarization state of the incident light is shown in Figure 5. The angle θ between the electric vector of light and the optically determined b axis of the crystal was allowed to vary between $-50°$ and 130° that is within the range of 180°. It is demonstrated that the interface medium (H_2O) shifts the positions of maxima for both strongly ($\lambda = 523$ nm) and weakly ($\lambda = 507$ nm) absorbed light. However, directions of the shift are opposite. Remarkably, the maximum reflectivity in both cases exhibits greater values than those recorded on the same crystal but in different runs for the reflectance spectra presented in Figure 3. The reason may be minor misalignment of the (001) crystal plane with respect to the electric vector of the incident light, finite reproducibility in fixing the angle $\theta(\pm 3°)$, structural inhomogeneities (the mosaic structure of the crystals) throughout the crystal surface, and, at last but not least, possible influence of its repeated contact with water. The differences in R not exceeding 15% make all the determined optical constants to be subject to an uncertainty between 6% and 30%.

The optical constants as a function of the angle θ between the electric vector of the reflecting light and the b crystal axis for $\lambda = 507$ nm are plotted in Figure 6. They have been obtained by the procedure given in Section 2A on the basis of direct experimental data displayed in Figure 5. Note that in contrast to k and ϵ, n, ε_i and ε_r show a strong gradient variation within a narrow θ range around $-5°$. Thus even small uncertainty in fixing θ can lead to a large scatter of the values of

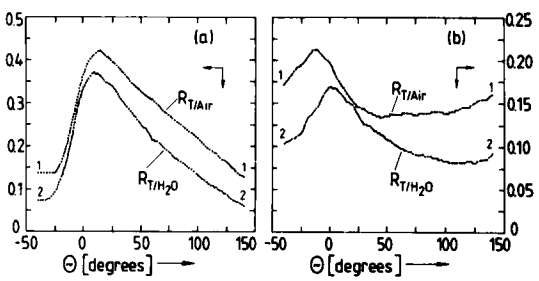

FIGURE 5 Reflectivity (R) in a tetracene crystal (50 μm thick) as a function of the angle θ between the electric vector of the reflecting, linearly polarized light and the b crystal axis. (*a*) strongly absorbed light with $\lambda = 523$ nm → $h\nu = 2.37$ eV; (*b*) weakly absorbed light $\lambda = 507$ nm → 2.46 eV. The spectra were taken from both the crystal/air ($R_{T/Air}$) interface (curves denoted by 1) and the crystal/water (R_{T/H_2O}) interface (curves denoted by 2).

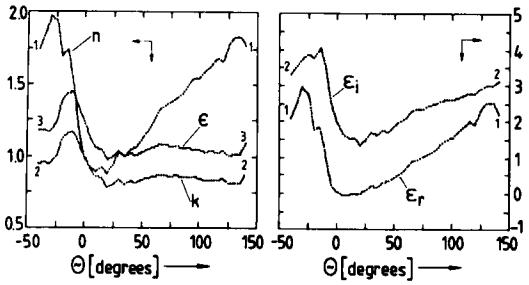

FIGURE 6 Optical constants as a function of the angle θ, determined from curves denoted by 1 in Figure 5 by TTM method; the ordinate for ε must be multiplied by a factor 2×10^5 cm^{-1}. The results obtained for light with $\lambda = 507$ nm.

these three constants and especially of the refractive index n. In our case for $\theta = \pm 3°$, $\Delta n \approx \pm 0.25$.

5. DISCUSSION

Based on our experimental data we come to the conclusion that the optical constants can be extracted from the narrow-range reflectance spectra of a crystal, taken from the reflecting surface being in contact with two different transparent media. The values of these constants for tetracene single crystal, derived from Equations (2–6), seem to be reliable, since some of them (for ϵ and n) are in good agreement with the more directly determined values given recently in Reference 8.

For comparison we have applied Kramers-Kronig relations for determination n, k and ε_r, ε_i and ϵ. The technique used here for evaluating the optical constants from normal incidence reflectance data on bulk material was set forth by Robinson.[10] Starting with the experimental curve $R = |r|^2$ versus E (where $E = h\nu$ is the energy in electron volts) and the Fresnel equation for normal incidence reflectance

$$r = |r|e^{i\vartheta} = \frac{n - ik - 1}{n - ik + 1} \tag{10}$$

the phase shift ϑ has been computed from the Kramers-Kronig relation between the real and imaginary parts of the complex function $\ln r = \ln|r| + i\vartheta$ which can be expressed in the form[11]

$$\vartheta(E_0) = \frac{1}{\pi} \int_0^\infty \frac{d \ln|r|}{dE} \ln \left| \frac{E + E_0}{E - E_0} \right| dE. \tag{11}$$

Then the complex number r can be related to the optical constants n and k by

separating the real and imaginary parts of Equation (10) yielding

$$n = \frac{1 - |r|^2}{1 + |r|^2 - 2|r|\cos\vartheta}$$
$$k = \frac{(n + 1)|r|\sin\vartheta}{|r|\cos\vartheta - 1}. \tag{12}$$

The integral for $\vartheta(E_0)$ is determined from a trapezoidal approximation as given is Reference 11 and employed in IBM 1620 and IBM 704 computer programs for determinations of optical constants from reflectance data.[12] The use of this technique for evaluating the optical constants implies that the reflectivity is known over the entire energy range. Since high-energy experimental values of R are not known an extrapolation for the high-energy values has been added in a way that the output from the computer agreed with the experimentally determined low-energy values. Figure 7 shows the results for different polarization states of the incident light. It is evident, on comparison with the results obtained by the two transparent media (TTM) method, that the values of all the optical quantities are generally lowered in the high-energy range of the spectra, leading to a blue shift of their main maxima. For instance a drastic difference can be seen in optical constants ε_r and ε_i (over a factor of 2), but also the often referred to refractive $n(\|b)$ and absorption $\epsilon(\|b)$ coefficients are smaller by about two times as compared with the TTM data.

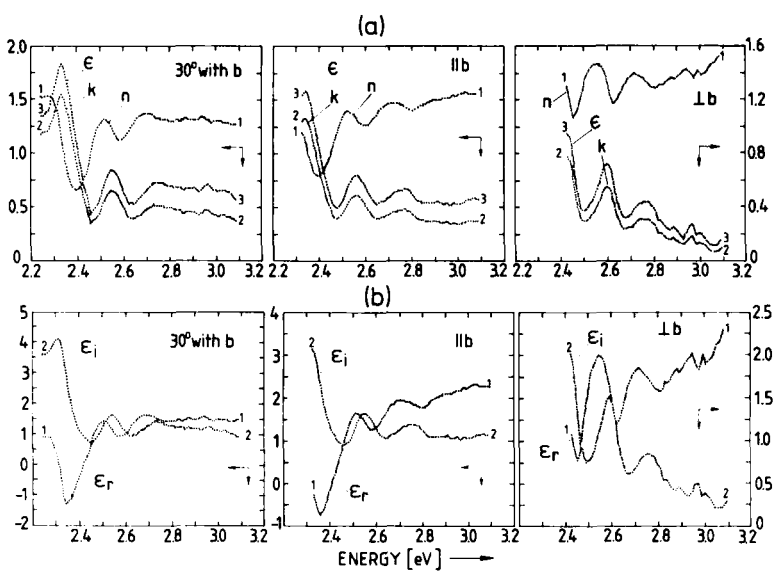

FIGURE 7 Optical constants versus photon energy for the tetracene single crystal as determined from the data of Figure 3 by the Kramers-Kronig procedure. The meaning and units of upper (*a*) and lower (*b*) parts of the figure are the same as in Figure 4.

One of the most unexpected results apparent in both Figure 4 and Figure 7 is that the absolute absorption maximum appears at energy ≈2.34 eV (λ = 530 nm), for the light with its electric vector deflected from the crystallographic *b* axis by a large angle amounting to 30°. The θ = 30° − absorption spectrum can be seen to follow the main features of the reflectivity which shows maximum at ≈2.36 eV (λ = 526 nm) for both θ = 30° and θ = 0° (cf. Figure 3). However, the reason for the highest reflectivity for θ = 30° seems to be an artefact since light at this photon energy penetrates the crystal down to its full crystal thickness, leading to an additional light flux reflected from the rear crystal surface. For this reason, optical constants determined here with θ = 30° do not reflect real material properties of tetracene crystal and should be verified by an analysis completed with multireflections within the crystal or measurements on a wedge-shaped crystal so that the light reflected from its rear surface could be directed out of the detection system. In both cases finite absorption in the crystal must be taken into account.

In spite of the above imperfection in the reflectivity measurements, the results obtained for optical constants of tetracene crystal as a function of θ with stronger absorbed light (Figure 6) show an apparent asymmetry with respect to the *b* axis direction. This is in contrast to anthracene crystal for which it was demonstrated that the absorption coefficient for the polarized light (4.6 eV) varies symmetrically as the electric vector of the light incident onto (001) face changes its orientation around the *b*-axis direction.[13] The difference is most probably due to the differences in structure of these two crystals. In the monoclinic structure of anthracene, the two molecules per unit cell are related by a glide plane parallel to the (*bc*) plane and they appear in a shallow herringbone pattern when viewed along the *a* axis. On the other hand, in the triclinic structure of tetracene, the only crystal symmetry operation is inversion; the transitions are not necessarily polarized along the crystallographic axes and can have oscillator strength in both the parallel to *b* and perpendicular to *b* directions (see References 9, 14).

The study of the reflectivity as a function of the orientation of the electric vector of light reflected from the single crystal surface can be a powerful tool in understanding of the defect modifications of the electronic properties of materials. The reflectance spectrum from a perturbed area $R_p(\bar{\nu})$ of the crystal differs from that from the unperturbed area $R_0(\bar{\nu})$ by a reduction in the specular reflectance intensity due to incoherent scattering (see *e.g.*, References 15, 16) and by an alteration in the shape of the band which is sharply reflected in the ratio spectrum $R_p(\bar{\nu})/R_0(\bar{\nu})$— a sensitive monitor of a band shape alteration. While such a ratio of the polarized reflectance spectra from a single crystal surface can be simply obtained by measuring $R_0(\bar{\nu})$ from one half of the crystal surface which is smooth (left physically unperturbed) and $R_p(\bar{\nu})$ from the other half which can be intentionally roughened or defected,[16] the measurement of the ratio spectrum in the case of crystalline films is more complicated since it requires independent determination of $R_0(\bar{\nu})$. Following the crystal reflectivity dependence on angle θ for various wavenumbers ($\bar{\nu}$) as a parameter (Figure 5 shows an example for two values of $\bar{\nu}$) one can obtain the reflectance spectrum averaged over the full-range of light polarization states which can be used as a measure of the reflectance from a perfectly smooth surface of (*ab*)-oriented tetracene films. Such an averaged spectrum is shown in Figure 8.

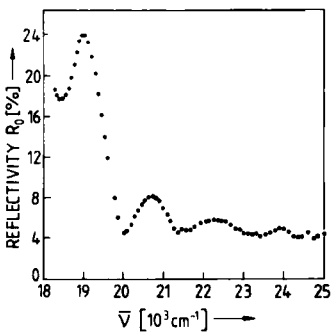

FIGURE 8 The polarization-averaged normal incident reflection spectrum from the (*ab*) face of a tetracene single crystal (50 μm thick).

Both the lowering of the reflectivity and nonexistence of Davydov splitting show up in the spectrum; such features are observed experimentally with reflectivity of crystalline thin tetracene layers and suggest at first glance the identity of the spectra. However a detailed comparison of these spectra by an analysis of the relative spectrum $R(\bar{\nu})/R_0(\bar{\nu})$ with the help of $R_0(\bar{\nu})$ given in Figure 8 shows that their shapes differ, the experimental spectrum from tetracene films being inhomogeneously broadened.[17] This supports a supposition that structural diagonal disorder is present not only in amorphous but also in near-surface regions of crystalline films deposited by vacuum evaporation onto rigid substrates.[17] It should be here pointed out that well-resolved Davydov splitting observed in the absorption spectra of crystalline tetracene films[17] does not settle a question of the type of structural disorder responsible for the shape of their reflectance spectra.

The well-resolved site energy splitting is considered as being the result of slightly perturbed structure corresponding to the weak-disorder case that is the case with Gaussian band broadening σ_D less than 0.3 of the half-exciton bandwidth B ($\sigma_D < 0.3$ B).[18,19] In contrast, the broad structureless spectra are interpreted in terms of the intermediate disorder type ($\sigma_D > 0.3$ B).[18–20] While the absorption spectrum reflects the structural disorder of the bulk of the sample and suggests that we are dealing with the weak-disorder case, its reflectance spectrum is characteristic of the near-surface region, where disorder is expected to be much stronger and the intermediate-disorder type of the structure cannot be excluded. Clearly, more spectroscopic work related to $R_0(\bar{\nu})$ is required to ascertain whether the intermediate-disorder type of structure exists in the surface regions of (*ab*)-oriented crystalline films of tetracene.

References

1. M. Pope and C. E. Swenberg, Electronic Processes in Organic Crystals, Clarendon Press, Oxford (1982).
2. Optical properties of Solids. Ed. by F. Abeles, North Holland, Amsterdam (1972).
3. M. Altarelli and D. Y. Smith, *Phys. Rev.*, **B9**, 1290 (1974).
4. G. Leveque, *J. Phys. C: Solid State Phys.*, **10**, 4877 (1977).

5. K. Jezierski, J. Misiewicz, J. Wnuk and J. M. Pawlikowski, *Opt. Appl.*, **11**, 571 (1981).
6. K. Jezierski, *J. Phys. C: Solid State Phys.*, **17**, 475 (1984).
7. K. Jezierski, *J. Phys. C: Solid State Phys.*, **19**, 2103 (1986).
8. K. Mizuno, A. Matsui and G. J Sloan, *J. Phys. Soc. (Jpn)*, **53**, 2799 (1984).
9. A. Bree and L. E. Lyons, *J. Chem. Soc.*, 5206 (1960).
10. T. S. Robinson, *Proc. Phys. Soc.*, **B65**, 910 (1952).
11. F. C. Jahoda, *Phys. Rev.*, **107**, 1261 (1957).
12. E. L. Kreiger, D. J. Olechna and D. S. Story (private information).
13. N. Geacintov and M. Pope, *J. Chem. Phys.*, **47**, 1194 (1967).
14. D. W. Schlosser and M. R. Philpott, *Chem. Phys.*, **49**, 181 (1980).
15. H. E. Bennet and J. O. Porteus, *J. Opt. Soc. Am.*, **51**, 123 (1961).
16. G. C. Morris and M. G. Sceats, *Mol. Cryst. Liq. Cryst.*, **25**, 339 (1974).
17. J. Godlewski, J. Kalinowski, S. Stizza, I. Davoli and R. Bernardini, *Thin Solid Films*, **146**, 115 (1987).
18. H. Bässler, *Phys. Stat. Sol. B*, **107**, 9 (1981).
19. R. Hesse, W. Hofberger and H. Bässler, *Chem. Phys.*, **49**, 201 (1980).
20. R. Jankowiak, K. D. Rockwitz and H. Bässler, *J. Phys. Chem.*, **87**, 552 (1983).